1 **Projected increases in wildfires may challenge regulatory curtailment of PM$_{2.5}$ over the**

2 **eastern US by 2050**

4 Chandan Sarangi[1,2]*, Yun Qian[2]*, L. Ruby Leung[2], Yang Zhang[3], Yufei Zou[4,2], Yuhang

5 Wang[4]

7 [1] Indian Institute of Technology Madras, Chennai, India

8 [2] Pacific Northwest National Laboratory, Richland, WA, USA

9 [3] Department of Civil and Environmental Engineering, Northeastern University, Boston, MA

10 [4] School of Earth and Atmospheric Sciences, Georgia Institute of Technology, Atlanta, GA,

11 USA.

14 *Corresponding Authors:

15 chandansarangi@iitm.ac.in

16 yun.qian@pnnl.gov

21   **Abstract**

22   Anthropogenic contribution to the overall fine particulate matter ($PM_{2.5}$) concentrations has

23   been declining sharply in North America. In contrast, a steep rise in wildfire-induced air

24   pollution events with recent warming is evident in the region. Here, based on coupled fire-

25   climate-ecosystem model simulations, summertime wildfire-induced $PM_{2.5}$ concentrations are

26   projected to nearly double in North America by the mid-21st century compared to the

27   present. More strikingly, the projected enhancement in fire-induced $PM_{2.5}$ (~ 1-2 $\mu g/m^3$) and

28   its contribution (~15-20%) to the total $PM_{2.5}$ are distinctively significant in the eastern US.

29   This can be attributed to downwind transport of smoke from future enhancement of wildfires

30   in North America to the eastern US and associated positive climatic feedback on $PM_{2.5}$ i.e.

31   perturbations in circulation, atmospheric stability and precipitation. Therefore, the anticipated

32   reductions in $PM_{2.5}$ from regulatory controls on anthropogenic emissions could be

33   significantly compromised in the future in the densely populated eastern US.

34   **Key points:**

35   1) Wildfire-$PM_{2.5}$ associations studied based on unprecedented two-way coupled fire-
36   climate-ecosystem model simulations
37   2) A steep rise in wildfire-induced air pollution events with recent warming is evident in
38   the region
39   3) The transported smoke from enhanced wildfires in North America can severely affect
40   air quality over Eastern US

41

42   **Keywords:** wildfire emissions, climate change, air quality, smoke transport, wildfire-climate-
43   ecosystem interactions

1. **Introduction**

Wildfires are widespread burning events in forests, shrub lands, and grazing lands. In North America (mainly Canada and the US), particulate matter emissions from wildfires are a significant source of regional air pollution (Shi et al., 2019; McClure and Jaffe, 2018; Van Der Werf et al., 2010; Jaffe et al., 2008). Since the 1980s, the number of large wildfires and the length of wildfire season have been increasing, and the trends are projected to continue in the future over the western US, Alaska and Canada (Kitzberger et al., 2017; Kirchmeier-Young et al., 2017; Abatzoglou and Williams, 2016; Partain et al., 2016; Jolly et al., 2015; Westerling et al., 2006; Gillett et al., 2004). Accordingly, particulate emissions from wildfires are also anticipated to increase in North America in the 21st century (Knorr et al., 2017; Liu et al., 2016; Val Martin et al., 2015). Human exposure to high concentrations of wildfire-emitted airborne particulate matter of diameter ≤ 2.5 μm ($PM_{2.5}$) is known to have substantial adverse effects on pulmonary and cardiovascular functioning (Anjali et al., 2019; Black et al., 2017), which contribute significantly to global and regional all-cause mortality (Zhang et al., 2020; Hong et al., 2019; Yang et al., 2019; Ford et al., 2018; Johnston. et al., 2012). Therefore, a better understanding of the future changes in wildfire-induced $PM_{2.5}$ and its contribution to the total surface $PM_{2.5}$ is essential.

In the last two decades, ambient air quality in the US has substantially improved due to a decline in $PM_{2.5}$ by ~ 40 % (US EPA, 2018). The decrease in $PM_{2.5}$ is primarily due to curtailment of anthropogenic emissions resulting from US-based efforts to meet regulations such as the Clean Air Act (US EPA, 2009), Cross-State Air Pollution Rule, Regional Haze Rule, and the motor vehicles emissions standards. Consequently, air quality over the contiguous US (CONUS) and Canada has improved steadily such that it is predicted to achieve the targeted National Ambient Air Quality Standards in the future (Nolte et al.,

68   2018). Under this promising scenario, the influence of wildfire-emissions on the total $PM_{2.5}$

69   becomes even more crucial. Depending on the competition between climate-induced increase

70   in wildfires and the regulatory control on anthropogenic emissions, future enhancement in

71   wildfire-induced $PM_{2.5}$ may compromise the reduction in anthropogenic $PM_{2.5}$ concentrations

72   in certain regions. In agreement, recent studies have highlighted the potential for future

73   enhancement in wildfire-induced pollution to diminish the reducing trend in $PM_{2.5}$, primarily

74   over the western US (O'Dell et al., 2019; Ford et al., 2018; Val Martin et al., 2015; Yue et al.,

75   2013).

76   While the fractional wildfire burnt area and fire intensities are the greatest over the

77   western US and Canadian regions within North America, anthropogenic emissions dominate

78   the ambient $PM_{2.5}$ concentration over the eastern US. The inherent geographical separation

79   between the regions with large wildfire emissions and anthropogenic emissions leads to a

80   pertinent question: will future enhancement in wildfires over the western US and Canada

81   have significant effects on $PM_{2.5}$ over the eastern US? Addressing this question is crucial

82   because the declining trend in $PM_{2.5}$ over the eastern US is the major contributor to the

83   observed 40% decrease in $PM_{2.5}$ over the US in the last two decades (US EPA, 2018).

84   Eastward advection of wildfire smoke from Canada and the western US has been found to

85   severely hamper the surface air quality of the central and eastern US under the influence of

86   the prevailing westerlies during the summer months (Brey et al., 2018; Wu et al., 2018;

87   Gunsch et al., 2018; Kaulfus et al., 2017; Dempsey, 2013). The transported wildfire smoke

88   can influence the meteorology and climate via the radiative impact of carbonaceous

89   emissions, changes in land albedo and cloud system perturbations (Ward et al., 2012; Liu et

90   al., 2014). These fire-weather interactions can have positive feedback on the locally-emitted

91    $PM_{2.5}$ in the eastern US by surface cooling and boundary layer suppression(Guan et al.,

92   2020). At the same time, fire-triggered ecosystem changes can induce negative feedback on

93   PM2.5 by reducing the future wildfires over North America (Zou et al., 2020). Thus, two-

94   way interactions between fires and climate that are important for predicting future changes in

95   wildfire locations, intensities, and durations (Harris et al., 2016) as well as associated

96   particulate emissions is essential. However, past studies have mostly employed simple

97   statistical models based on statistical regressions of present-day fire burnt area on the

98   meteorological fields (Liu et al., 2016; Spracklen et al., 2009; Yue et al., 2013; Val Martin et

99   al., 2015), and more recently, one-way coupled modelling (Ford et al., 2018; O'Dell et al.,

100   2019).

101   Here, based on new two-way coupled fire-climate-ecosystem simulations, we

102   demonstrate the significance of wildfire-induced contributions to ambient PM$_{2.5}$ over the

103   eastern US due to enhanced wildfire smoke transportation and smoke-induced changes in

104   weather in eastern US. This enhancement in wildfire-induced PM$_{2.5}$ may potentially challenge

105   the targeted policy-driven reduction of PM$_{2.5}$ in the eastern US. Next, our model setup,

106   experiments and methodology are explained in Section 2, followed by results and discussion

107   in Section 3. The study is summarized in Section 4.

108   **2. Materials and Methods**

109   **2.1. RESFire-CESM Model description**

110   We employ the open-source REgion-Specific ecosystem feedback fire (RESFire)

111   model coupled with the Community Land Model version 4.5 and the Community

112   Atmosphere Model version 5 (CAM5) of the Community Earth System Model (CESM)

113   version 1 (Zou et al., 2019; Neale et al., 2013) to perform two-way coupled simulations.

114   RESFire provides state-of-the-art capabilities to simulate the complex fire-climate-ecosystem

115   interactions globally for fires occurring over wildland, cropland, and peatland. Although

116   wildfires dominate in the North American region, RESFire simulates both wildfires and

117 prescribed fires. Moreover, this integrated setup includes climatic feedback from fire-induced

118 aerosol direct and indirect radiative effects and associated weather changes. It also includes

119 feedback from fire-induced vegetation distribution changes and associated biophysical

120 processes such as evapotranspiration and surface albedo. Sofiev et al. (2012) described the

121 fire plume rise parameterization. Other features in CLM4.5 and CAM5, such as the

122 photosynthesis scheme (Sun et al., 2012), the MAM3 aerosol module (Liu et al., 2012), and

123 the cloud macrophysics scheme (Park et al., 2014), allow for more comprehensive

124 assessments of the climate effects of fires through their interactions with vegetation and

125 clouds. Fire-ecosystem interactions are modelled by simulating fire-induced vegetation

126 mortality and regrowth (and associated land cover change) in RESFire. This approach has

127 been introduced in Zou et al. (2019) and the simulated ecological and climatic effects of

128 wildfires have been evaluated in two sets of sensitivity experiments in Zou et al. (2020).

129 Although fire-climate-ecosystem interactions are considered in this study, our focus is on the

130 fire-induced changes in $PM_{2.5}$ over Canada and the US, so the two vegetation-focused

131 sensitivity experiments reported in Zou et al. (2020) are not included in this paper. Please

132 refer to Zou et al. (2019) and Zou et al. (2020) for more details about the simulation of fire-

133 ecosystem interactions.

134 **2.2 Numerical Experiment and Methodology**

135 We designed two sets of simulations for the present day and future scenarios to

136 quantify the impacts of fire-climate-ecosystem interactions (Table 1). The spatial resolution is

137 $0.9°$ (lat) $\times 1.25°$ (lon) with a time step of 30 min. In each set of simulations, we conducted a

138 default all emission included control run (X_{ALL}, where x=2000 or 2050 indicates the present

139 day or future, respectively) and a sensitivity run with no wildfire emissions to the atmosphere

140 (X_{WEF}, where X is the same as for the control runs). The ALL runs are designed to simulate

141 fully interactive fire disturbances such as fire emissions with plume rise and fire induced land

142   cover changes of the present day (representative of the 2000s, 2000ALL) and a moderate future

143   emission scenario (representative of the 2050s, 2050ALL) via the RCP4.5. The only difference

144   between the ALL and WEF scenario is that wildfire emissions are absent in the WEF

145   scenario. Specifically, in the WEF runs, the online simulated fire emissions are not passed to

146   the CAM5 atmosphere model so that the difference between the ALL and WEF runs can be

147   used to isolate the atmospheric impacts of fire-climate interactions.

148   Table 1: Summary of the sensitivity simulations performed

Scenario	Present-day		Future	
Experiment Name	2000_{ALL}	2000_{WEF}	2050_{ALL}	2050_{WEF}
Simulation years	2001-2010	2001-2010	2051-2060	2051-2060
Atmosphere	CAM5	CAM5	CAM5	CAM5
Land	CLM4.5	CLM4.5	CLM4.5	CLM4.5
Ocean	Climatology	Climatology	RCP4.5	RCP4.5
Sea ice	Climatology	Climatology	RCP4.5	RCP4.5
Non-fire emissions	ACCMIP	ACCMIP	RCP4.5	RCP4.5
Fire emissions	Online fire aerosols with plume rise	—	Online fire aerosols with plume rise	—
Land cover	Fire disturbances on present-day condition	Fire disturbances on present-day condition	Fire disturbances on RCP4.5 condition	Fire disturbances on RCP4.5 condition

149

150   For the present-day experiments, we used the spun-up states from Zou et al. (2019) as

151   initial conditions for both meteorological and chemical variables. Sea surface temperature

152   (SST) for the present day was obtained from the Met Office Hadley Centre (HadISST).

153   Present-day non-fire emissions from anthropogenic and other sources were based on

154   ACCMIP (Lamarque et al., 2010) for the year 2000. We replaced the prescribed GFED2 fire

155   emissions (van der Werf et al., 2006) in the default setting of CESM with the online-coupled

156   fire emissions generated by the RESFire model. Zou et al. (2019) provided more details of

157   the physics parameterizations and modeling experiment settings used in these simulations.

158   Land use and land cover data for 2000 and 2050 from the Land-Use History A product (Hurtt

159   et al., 2006) are used to initialize the $2000_{ALL}/2000_{WEF}$ and $2050_{ALL}/2050_{WEF}$ simulations,

160   respectively. Following the above setup, the future scenario 2050_{ALL} experiment accounts for

161   both fuel load changes associated with the projected land use and land cover change

162   (LULCC) in the 2050s and fire weather changes driven by the SST and sea ice forcing from a

163   coupled CESM simulation following the greenhouse gas (GHG) forcing of the RCP4.5

164   scenario. The global mean GHG mixing ratios in the CAM5 atmosphere model were fixed at

165   the year 2000 levels in all the present-day experiments and they were replaced by those of the

166   RCP4.5 scenario with the well-mixed assumption and monthly variations. However, the

167   future population and socioeconomic conditions were identical to those of the present day so

168   there was no explicit impact of human-induced mitigation/enhancement effects on wildfires

169   in the future projection in all the future experiments. Future human impacts were considered

170   implicitly in LULCC-induced fuel load changes in the RCP4.5 scenario.

171   The net projected changes by 2050s in emissions, meteorology and air quality during

172   summer (JJA: June, July, August) months are estimated by comparing decadal-mean values

173   simulated by 2000_{ALL} with 2050_{ALL}. Wildfire-induced enhancement in $PM_{2.5}$ concentration in

174   the present day and mid-21st century is estimated by comparing 2000_{ALL} with 2000_{WEF} and

175   2050_{ALL} with 2050_{WEF}, respectively. Further, the projected increase in wildfire-induced

176    $PM_{2.5}$ in the future is calculated by comparing the simulated wildfire effect of the 2050s

177    $(2050_{ALL}-2050_{WEF})$ with that of the 2000s $(2000_{ALL}-2000_{WEF})$. With large spatiotemporal

178   variability, the projected changes in transported fire-emissions from the western US and

179   Canada to the eastern US by the 2050s and the corresponding impacts are summarized using

180   probability distribution functions. The latter provide information not only for the mean but

181   also variability and extreme values to quantify the simulated changes for the three subregions.

182

3. Results and Discussion

3.1 Model Evaluation

Zou et al. (2019) performed comprehensive evaluation of the RESFire simulated wildfire burnt area distribution, associated carbon emissions and terrestrial carbon balance to demonstrate reasonable model skill. Zou et al. (2020) compares global fire simulations by CESM-RESFire with modeling results reported in the literature to show better agreement with the GFED4.1s benchmark data and predicts more prominent changes in the future than those predicted by Kloster et al. (2010, 2012). These differences might come from differences in the climate sensitivities of the fire models and scenarios and other input data used to make future projections.

Here, we evaluate the simulated surface $PM_{2.5}$ against satellite-estimates (Figure 1) over North America. The $PM_{2.5}$ concentration is calculated as the sum of sulfate, nitrate, fine sea salt (first 2 size bins), fine dust (first size bin), black carbon (BC), and organic aerosol (OC) at the surface-level of model. OC is the sum of primary organic matter (POM) and secondary organic aerosol (SOA), and SOA is the sum of secondary species formed from toluene, monoterpenes, isoprene, benzene, and xylene. Figure 1 compares the observed and simulated mean annual $PM_{2.5}$ averaged over 2001-2010. The 10-year average satellite AOD-derived annual mean surface $PM_{2.5}$ concentrations (Van Donkelaar et al., 2018) are regridded to the model grid (Figure 1A) and then compared with the RESFire simulations in the 2000_{ALL} present-day run (Figure 1B). The spatial distribution of annual surface $PM_{2.5}$ is reasonably well simulated but also have some biases. To quantify the biases, we also estimated the correlation coefficient as well as normalized mean biases (NMB) of the simulated values compared against the satellite retrieved values over two subregions. Quantitatively, the NMB values over the western US (WUS) and eastern US (EUS) are 18% and 7%, respectively (Figure 1C-D). In addition, the spatial variability of the 2001-2010

averaged annual AOD distribution (Supplementary Figure 1) is also well represented in our

simulation, although the model underestimates high AOD values. Similar spatial variability

and biases in AOD and $PM_{2.5}$ were also found when a comparison was performed for only

summer months (June through August; JJA). The simulated $PM_{2.5}$ has also been evaluated

against the ground-based Interagency Monitoring of Protected Visual Environments

(IMPROVE) data, showing similar spatial pattern and biases (10-25%) (Supplementary

Figure 2). The biases are smaller over Eastern US and Southwestern US region. The

simulated PM2.5 values over California matches quite well with the observed annual mean

values. However, the biases over Northwestern US region are ~30-40%, a portion of which

could be attributed to possible biases in model's meteorology in northwestern US region.

Nonetheless, both satellite and in situ evaluation indicate that our simulation biases are

largely within the uncertainty range among the various satellite and ground-based datasets,

which have normalized mean biases ranging from -3.3% to 33.3% when benchmarked against

the ground-based IMPROVE data over the contiguous US (Diao et al., 2019; Val Martin et al.

(2015)).

      Discrepancies between the simulated and observed $PM_{2.5}$ values may be attributed to

several potential reasons. First, the satellite-derived data has a non-zero lower bound of $PM_{2.5}$

concentrations, so the ambient background concentrations for relatively cleaner regions such

as the western US may be overestimated (Figure 1C), also the sampling frequency between

these datasets are different. Second, year 2000-based constant non-fire emissions were used

in the RESFire simulation, which may result in overestimation of the $PM_{2.5}$ concentrations

from non-fire sources during 2001-2010 when anthropogenic emissions and $PM_{2.5}$

concentrations continue to decrease (US EPA, 2018). This overestimation is prominent in

regions dominated by non-fire sources such as the southeastern US. Third, large uncertainties

in fuel consumption and emission factors preclude an accurate estimation of the primary fire

233 emissions in the model, especially for the eastern US where large fractions of low-intensity

234 prescribed fires consume only under-canopy fuels such as litter and duff layers. The fire

235 model may fail to capture the subtle distinctions between low-intensity prescribed fires and

236 forest fires, so more fuels are consumed and result in higher emissions. Lastly, comparison of

237 a coarsely resolved simulation against in-situ observations also contributes to uncertainty.

238 Differences in the degree to which fire-climate interactions and other physical processes and

239 feedbacks are represented by the models can explain the slights differences in estimating the

240 present day mean wildfire-induced change in $PM_{2.5}$ over local and downwind regions

241 between our simulations and previous studies. Nonetheless, reasonable simulation of the

242 spatial distribution of wildfire burnt area, AOD, and near surface particulate concentration

243 (mean bias of ~10-20 %) instills confidence about the fidelity of our model setup in

244 particulate pollution simulation, which is the focus of this study.

245

246
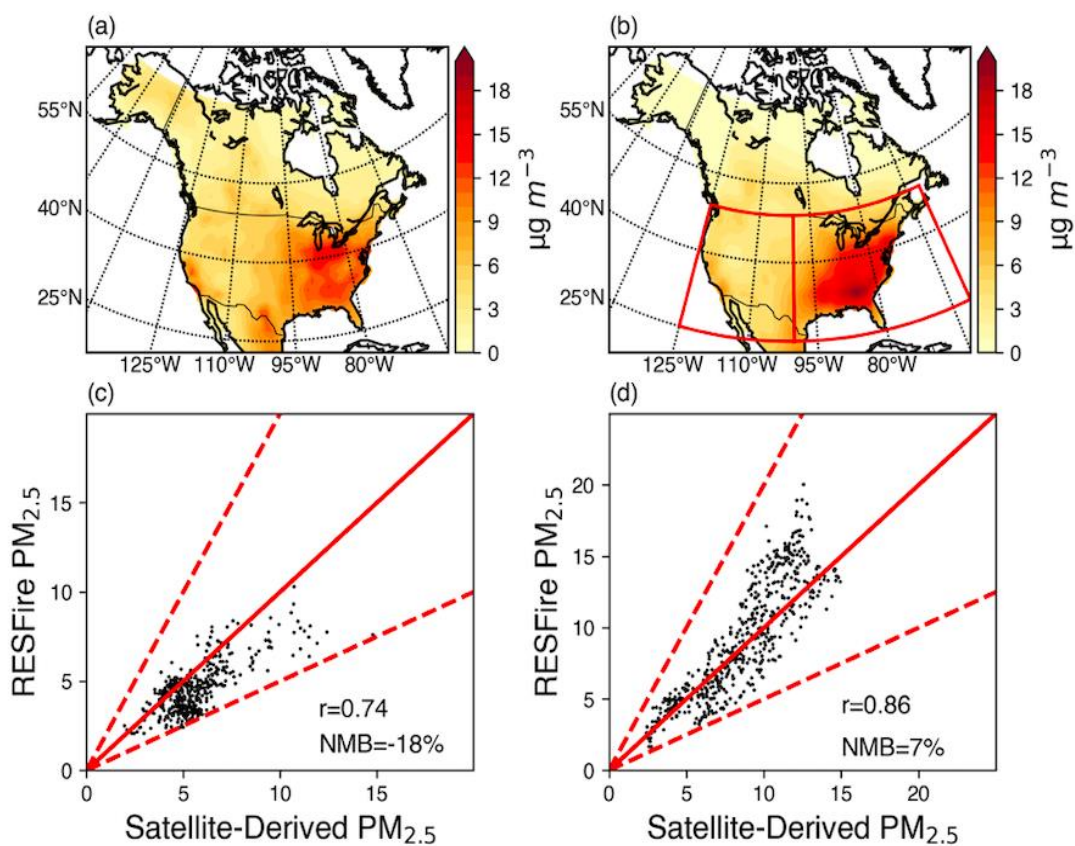
Figure 1: Comparison of the 10-year (2001-2010) averaged annual mean surface $PM_{2.5}$ concentration between observations and RESFire simulations. (a) Satellite-derived surface $PM_{2.5}$ concentrations (with dust and sea-salt removed) estimated by Donkelaar et al., 2018 (available at https://sedac.ciesin.columbia.edu/data/set/sdei-global-annual-gwr-pm2-5-modis-misr-seawifs-aod; last access: 5 November, 2021); (b) 2000_{ALL} Simulated surface $PM_{2.5}$ concentrations (with dust and sea-salt removed) averaged over 2001-2010; The red boxes denote the two subregions (EUS and WUS) shown in Fig. 2 in the main text. (c) comparison of simulated and satellite based gridded surface $PM_{2.5}$ concentrations in the WUS subregion; Number of samples is equal to the number of land grids ~450 (d) same as (c) but in the EUS subregion. Number of samples is equal to the number of land grids ~375 The red solid and dashed lines denote the 1:1 ratio line and $\pm$100% biases, respectively. The correlation coefficients and NMB values are shown at the lower-right corner of each subplot.

3.2 Fire-induced changes in burnt area and $PM_{2.5}$

The decadal-mean annual fire burnt area simulated for the present day shows widespread wildfires over the entire North America (Figure 2A). Specifically, Canada and the forested areas of the northwestern (> 36 N latitude) and southeastern (< 36 N latitude) US are most intensely affected by wildfires in the present day. By the mid-21st century, a striking increase of 2-5 times in fire burnt area is projected over Canada, Alaska, the Pacific Northwest and portions of the western US by the 2050s (Figure 2B). A distinct positive shift in the probability density function (PDF) of annual fire burnt area is evident in the future, with the decadal-mean difference statistically significant at the 99% confidence level (Zou et al., 2020). A small and statistically insignificant change in interannual variability (~ 0.4 Mha yr^{-1}) of fire burnt areas is also simulated between the present and future. Specifically, our model predicts more than a doubling of burnt area in boreal regions of Canada in the future, in line with a previous projection for Canada (Wotton et al., 2017). Future enhancement in fire burnt area is ~ 20-50% in most fire grids over the western coast of US, which is higher than that over the eastern US (Figures 2A and 2C). The increase over the western US is closer to the lower bound of that derived from statistical model ensemble projections for the western US in the mid-21st century (Yue et al., 2013). The statistics-based projections of future burnt

277 area over North America were likely too high because fire-induced land cover change, fuel

278 load reduction and factors could induce a negative fire feedback, which was not considered in

279 previous fire projection studies (Zou et al. 2020).

280 Annual fire burnt area in the southeastern US shows a decline in the future (Figure

281 2C), as precipitation is projected to increase in that region (discussed later). Note that all

282 future fire changes between 2050_{ALL} and 2000_{ALL} are primarily associated with climate

283 warming in response to the increase in greenhouse gas (GHG) concentrations in the RCP4.5

284 scenario. No direct impacts of population and socioeconomic changes on wildfires are

285 included in our simulations, although these factors contribute to changes in GHG emissions

286 (via the RCP scenario) that influence the climate simulated in 2000_{ALL} and 2050_{ALL}. As about

287 80% of the projected fire changes in the future is restricted to the summer season (June

288 through August; JJA) (Figure 2D), we focus on analysis of the summer-mean wildfire-

289 induced $PM_{2.5}$ and its projected future changes over North America.

290
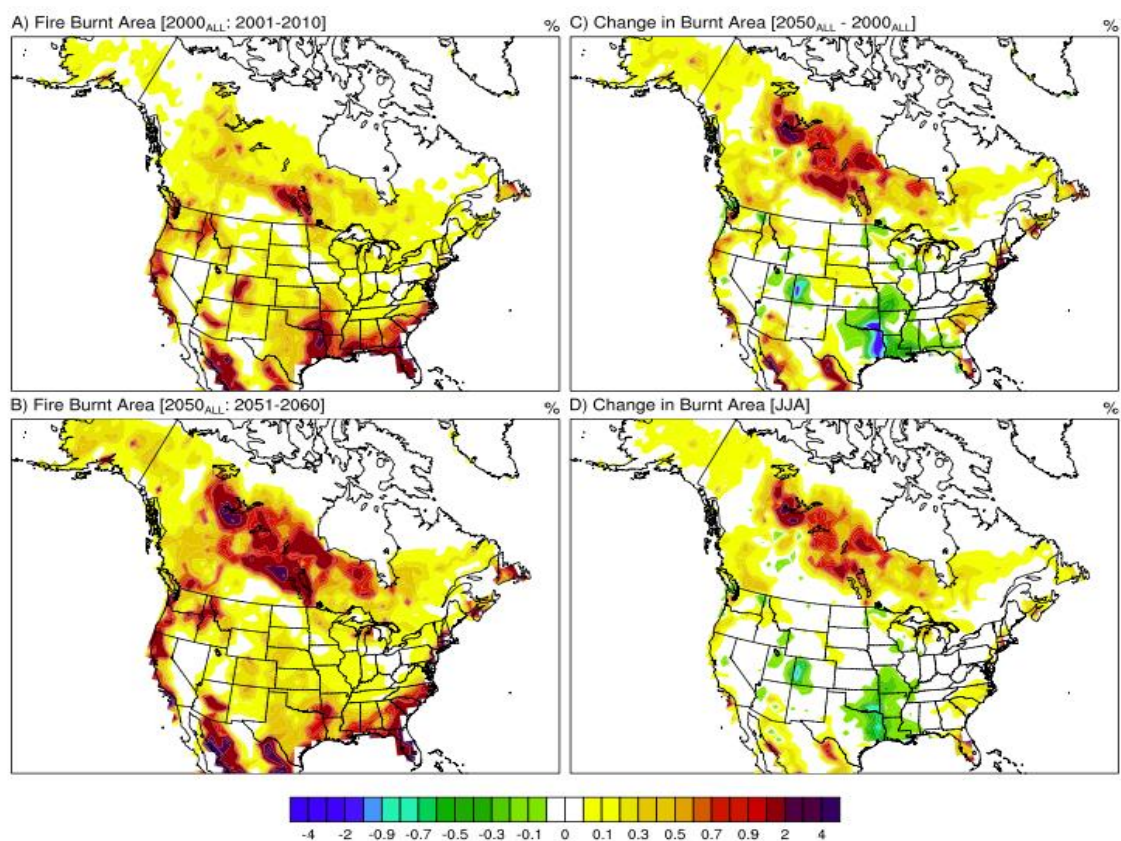
Figure 2: **Spatial distribution of fire burnt area. A-D**, Spatial distribution of simulated decadal-mean annual burnt area (as percentage) over North America for present day (A), mid-21st century (B) and the net change between the 2050s and the 2000s (C). **D**, same as (C), but for wildfire burnt area during summer only (June through August; JJA). The colorbar illustrate grid fraction of area burnt.

The simulated 10-year averaged summer-mean wildfire-induced PM$_{2.5}$ values in 2000$_{ALL}$ are more than 0.5 µg/m^3 over a large part of North America in the present day, with noticeably larger values (> 1 µg/m^3) in Canada and the northwestern, central, and southeastern US (Figure 3A). Interestingly, the spatial distribution of wildfire-induced PM$_{2.5}$ > 1 µg/m^3 resembles an inverted horse-shoe shape. The inverted horse-shoe shaped spatial distribution is also consistent with the wildfire-smoke climatology derived from the satellite-guided operational smoke product of the Hazard Mapping System (HMS) during 2005-2015 (Brey et al., 2018; Kaulfus et al., 2017). By the mid-21st century, the spatial extent of the horse-shoe shape for areas with wildfire-induced PM$_{2.5}$ enhancement > 1 µg/m^3 expands significantly to span most regions of North America, with the most pronounced enhancement occurring over Canada (Figure 3B). The PDFs of the spatial distribution for the three regions can be seen in Figure 3C-E. Specifically, wildfire induced PM$_{2.5}$ in the 2000s over Canada, WUS and EUS during summer is ~ 1-3 µg/m^3, 1-3 µg/m^3 and 0.6-1.2 µg/m^3, respectively. Maximum values within the WUS region are found over the Pacific Northwest, with most areas having wildfire induced PM$_{2.5}$ values of ~ 2-3 µg/m^3. Similarly, the southern states have relatively high wildfire induced PM$_{2.5}$ concentrations of ~ 2-4 µg/m^3 within the EUS in the present-day simulation.

Compared to the 2000s, the wildfire induced JJA-averaged PM$_{2.5}$ values are almost doubled to ~ 3-6 µg/m^3 over Canada in the 2050s (Figure 3B and Figure 3C). Consistently, the values of wildfire induced PM2.5 over WUS (mainly coastal) also doubled in 2050s compared to 2000s, with modal values of ~ 2-2.5 µg/m^3 (Figure 3D). Most interestingly, the enhancement in wildfire-induced summer-mean PM$_{2.5}$ over the northern EUS is also

319 significant by the 2050s (Figures 3B). Largely, the summer-mean wildfire-induced PM2.5

320 concentration over EUS increases from ~0.8 to ~2 $\mu g/m^3$ in the mid-century to values of 1.2-

321 3.0 $\mu g/m^3$ (Figure 3E). The summer-mean wildfire-induced PM2.5 is thus projected to double

322 in North America by the 2050s compared to the 2000s, with a substantial coverage over the

323 EUS. An important finding from these PDFs appears to be that there are fewer grids with < 1

324 $\mu g/m^3$ wildfire induced PM2.5, or alternatively, that more regions are being influenced by

325 PM2.5, and many areas that were already seeing wildfire impacts are seeing enhanced

326 impacts. Such enhancement is found not only at the surface but also in an elevated

327 atmospheric layer over EUS between 900 and 700 hPa. This is nonintuitive given the fact that

328 the increase in fire-burnt area by mid-century over the EUS is not substantial.
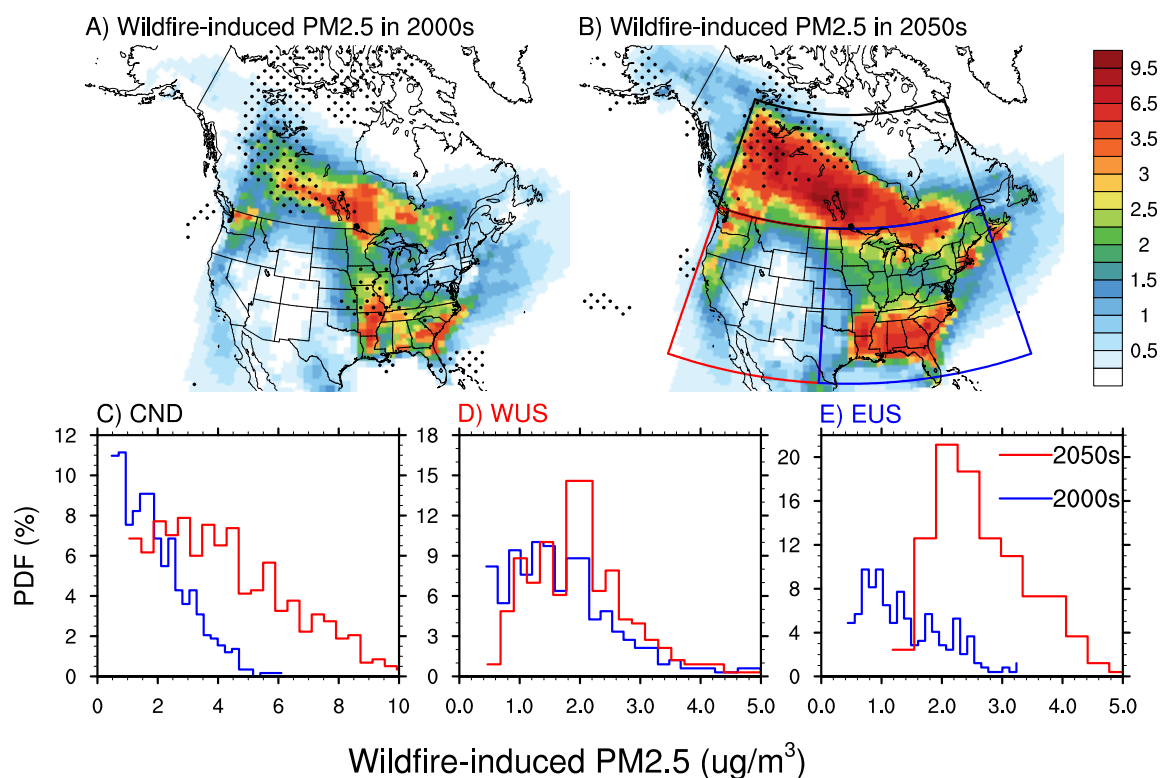
329

330 Figure 3: **Spatial distribution of** PM2.5 **concentrations.** Spatial distribution of decadal-mean
331 wildfire-induced enhancement in summer (June through August; JJA) PM2.5 concentration
332 over North America for present day (A, 2000ALL-2000WEF) and future (B, 2050ALL-2050WEF).
333 The grids with statistical significance of 90% is identified by black dots. **C-E**, Probability
334 density functions (PDFs) of wildfire contribution within the three regions shown in Figure 2B

335 for Canada (CND: black box) (C), WUS (red box) (D), and EUS (blue box) (E), respectively, for

336 2000s (blue) and 2050s (red). Only grids over land in North America are used to generate

337 the PDFs. The y-axis indicates the probability of occurrence of different $PM_{2.5}$ values shown

338 in the x-axis. The colorbar illustrates PM2.5 in ug/m^3.

339

340   As anthropogenic- and wildfire-induced $PM_{2.5}$ concentrations may change differently

341 with time across North America, next, we investigate the relative contribution of wildfire-

342 induced $PM_{2.5}$ to the total $PM_{2.5}$ in the future. Prominent enhancement of the wildfire

343 contribution is apparent in the entire domain by the 2050s (Figures 4A-B). Largely, during

344 the 2000s, the simulated fractional contribution of wildfires to $PM_{2.5}$ is ~15-50 % in Canada

345 (Figure 4A). Specifically, a bi-modal distribution is simulated over Canada with modal values

346 around 18% and 30% (Figure 4C). Over WUS, the present day simulated percentage

347 contributions of wildfire-induced values are 5-25% (Figure 4A), with modal values between

348 10-20% (Figure 4D). Note that many areas located in the Pacific Northwest have higher

349 values of ~30-40% (Figure 4A). At the same time, the fractional contribution by wildfire-

350 induced $PM_{2.5}$ is ~5-10% in most areas of EUS in present day (Figure 4F). Nevertheless,

351 some areas in the central US also have higher values of ~10-25% (Figure 4A).

352
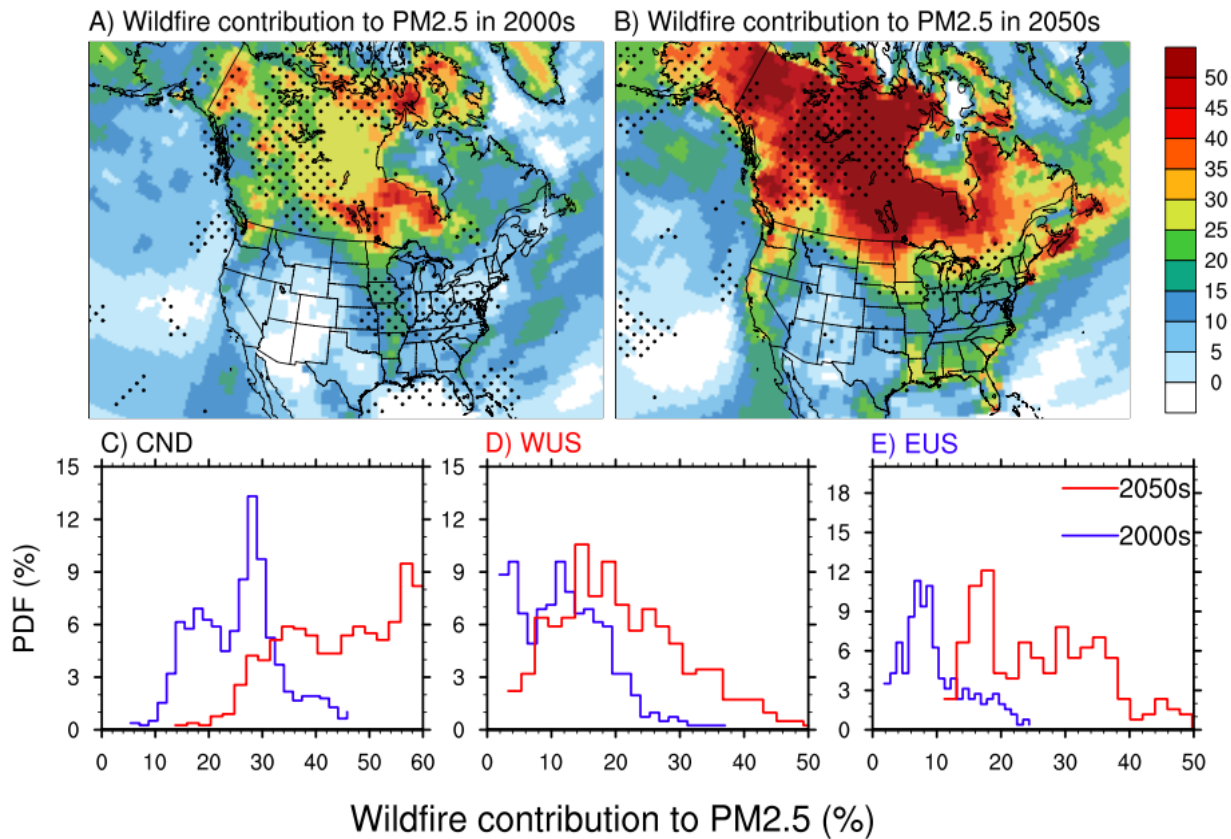
Figure 4: **Spatial distribution and probability density function of the percentage contribution of wildfire emissions. A-B**, Spatial distribution of the percentage contribution of wildfire emissions to decadal-averaged summer (June through August; JJA) mean $PM_{2.5}$ concentrations over North America during present day (A) and future (B). The percentage contribution of wildfire-induced $PM_{2.5}$ to the total $PM_{2.5}$ concentrations is calculated as $([2000_{ALL}-2000_{WEF}]/2000_{ALL})$ and $([2050_{ALL}-2050_{WEF}]/2050_{ALL})$ for the present and future, respectively. The grids with statistical significance of 90% is identified by black dots. **C-E**, Probability density functions (PDFs) of the percentage wildfire contribution within the three regions shown in Figure 2D for Canada (CND: black box) (C), WUS (red box) (D), and EUS (blue box) (E), respectively, for the 2000s (blue) and the 2050s (red). Only grids over land in North America are used to generate the PDFs. The y-axis indicates the probability of occurrence of different $PM_{2.5}$ values shown in the x-axis.

The wildfire contributions in the 2050s show a clear shift towards higher values in all sub-regions compared to the 2000s (Figure 4B). Over Canada, the values shifted from 15-30 % in the 2000s to ~30-60% in the 2050s, a nearly two-fold increase in the fractional contribution of wildfire emissions to the total $PM_{2.5}$ concentration is simulated (Figure 4B

370 and corresponding PDF in Figure 4C). Similarly, the contribution values increased to ~ 10-35

371 % in the 2050s, compared to 10-20% in the 2000s over WUS (Figure 4B), thereby featuring a

372 broadening of the bi-modal distribution of wildfire contribution (Figure 4D). The shift in the

373 percentage contribution is most prominent for the higher values, corresponding to some areas

374 located in the Pacific Northwest and west coast of the US (Figure 4B). Consistent with Figure

375 3B, the shift in the contribution values over EUS is also very distinct, revealing an increase in

376 the mode values from 6-10% in the 2000s to ~16-20 % by the 2050s (Figure 4B and Figure

377 4E). Thus, not only in absolute values, but our results also underscore a large increase in the

378 contribution of wildfire emissions over EUS in the future.

379 **3.3. Mechanistic understanding of the underlying processes**

380 The larger enhancement in the relative contribution of wildfire emissions to the total

381 surface $PM_{2.5}$ in EUS in the 2050s can be explained by three mechanisms. First, due to the

382 increase in Canadian and western US wildfires, downwind transport of wildfire smoke

383 plumes to EUS will be enhanced by the 2050s. This long-range transport to the atmospheric

384 column of EUS can happen within a few days of the fire occurrence (Supplementary Figures

385 3A and 3B). Using Hazard Mapping System (HMS)-detected smoke plumes, recent studies

386 identified a strong positive association between the transported smoke plumes in the

387 atmospheric column and collocated surface PM2.5 enhancement in EUS (Brey et al., 2018;

388 Wu et al., 2018; Gunsch et al., 2018; Kaulfus et al., 2017; Larsen et al., 2017; Dempsey,

389 2013). Hazard Mapping System (HMS) is an operational smoke detection product over North
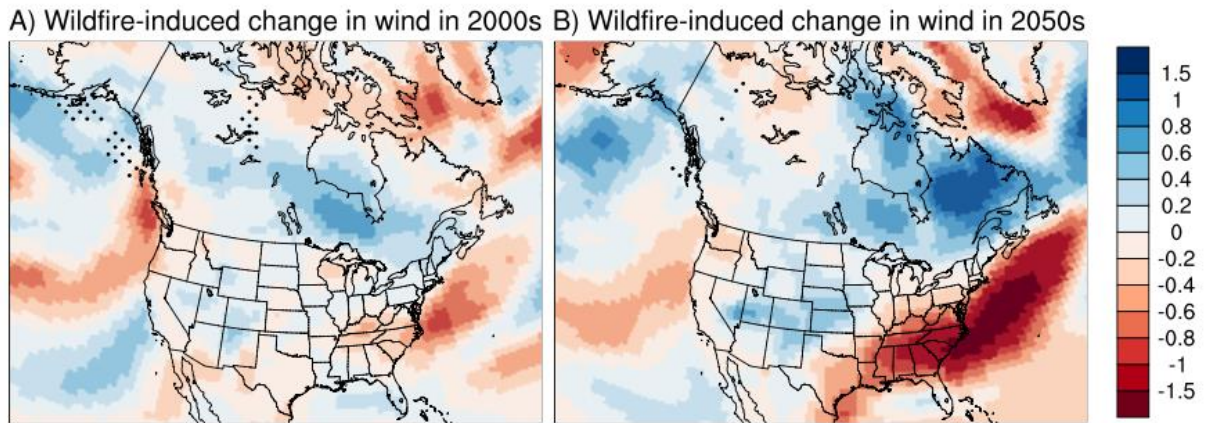
Figure 5a: Spatial distribution of decadal mean summer (June through August; JJA) wildfire-induced future changes [(2050_ALL-2050_WEF) – (2000_ALL-2000_WEF)]. A) Wind speed below 850 hpa for [(2050_ALL- – 2000_ALL], B) Wind speed below 850 hpa [(2050_WEF) – (2000_WEF)]. The unit is m/s. The grids with statistical significance of 90% is identified by black dots.

America known as developed by the National Oceanic and Atmospheric Administration

(NOAA) and operated by National Environmental Satellite, Data, and Information Service

(NESDIS), available at http://satepsanone.nesdis.noaa.gov/FIRE/fire.html. Specifically, these

studies found that the smoke plumes transported from Canada are located at an altitude of ~

1-3 km over EUS (Colarco et al., 2004; Wu et al., 2018). Due to mixing by the daytime

boundary layer and deposition, the smoke plumes enhance the surface PM$_{2.5}$ concentration

over EUS (Wu et al., 2018; Colarco et al., 2004; Rogers et al., 2020; Dreessen et al., 2015).

Hence HMS smoky days may be a useful proxy for wildfire-induced surface PM2.5 over

North America. In agreement, Brey et al. (2018) showed that the HMS-based smoke plumes

observed over EUS is significantly aged, suggestive of their long-range transport origin.

Consistent with the observed temporal change in HMS pattern, Xue et al. (2021) estimated

using the mid-visible Multi Angle Implementation of Atmospheric Correction (MAIAC)

satellite-derived Aerosol Optical Depth (AOD) that Canadian and western US fires have

caused an increase in the daily PM2.5 over Montana, North Dakota, South Dakota and

Minnesota by 18.3, 12.8, 10.4 and 10.1 $\mu g\ m^{-3}$, respectively, between August 2011 (a low

fire month) and August 2018 (a high fire month). In summary, the visually apparent satellite-

based signatures of wildfire-smoke across Canada and EUS provide a necessary, though not

sufficient, support for the influence of Canadian smoke plumes on EUS air quality. Although,

the change in burnt area over northeastern EUS is negligible compared to the western US and

Canadian regions, however, there are some enhancements seen over east coast of US, which

can also contribute to enhanced fire emissions.

In future, the wildfire-induced change in speed of the westerly jet flows over Canada

wildfire regions is increased (Figure 5 A-B). It indicates that the westerly-induced transported

wildfire emissions from Canada boreal forests to the eastern half of Northern America and

EUS will be enhanced in future compared to that in present era. On the one hand, the

wildfire-induced changes in wind speed over the EUS is reduced in future, which implies that

the local emissions over EUS are less dispersed. Simultaneously, this will also cause the

transporting smoke plumes to slow down and be subjected to relatively more boundary layer

mixing over the EUS and dry deposition/settling enhances, thereby contributing to the

enhanced PM2.5 values at surface. The westerly winds over western US below 40° N is also

strengthened in future (Figure 5 A-B) compared to present day which indicates more

advection flux wildfire emissions to EUS. Thus, the net effect is more removal of wildfire-

emitted PM2.5 from WUS and more influx of wildfire-emitted PM2.5 in EUS.

Along with this dynamical changes, other climatic feedbacks simulated can also contribute to

enhancement of EUS pollution. Specifically, the enhancement of wildfire-induced smoke

aerosols increases solar absorption and scattering in the future (Figure 6A). This reduces the

incoming solar radiation reaching at the surface (Figure 6B) and induces surface cooling.

With atmospheric warming and surface cooling, lower-tropospheric stability is enhanced by

wildfire aerosols in the future (Figure 6C). The smoke plumes which reaches eastern US are

at an elevated altitude due to self-lofting property of absorbing aerosols as they travel

435 downwind but the smoke over western US is at near surface elevation as it is at its source

436 region. This can explain the more significant atmospheric stability simulated over the eastern

437 US compared to the source regions in western US and boreal forests of Canada. Relatively

438 stronger atmospheric stability over eastern US impose a stronger thermal capping that traps

439 more anthropogenic aerosols and particulate matter near the surface over EUS (already an

440 emission hotspot). At the same time, future increase in wildfire emissions also leads to

441 greater reduction of monthly rainfall (Figure 6D) over EUS, which may additionally

442 strengthen the positive feedback to surface PM$_{2.5}$ over EUS by reducing wet scavenging of

443 transported wildfire smoke to EUS. Thus, wildfire-emitted aerosols induce positive feedback

444 on the surface PM$_{2.5}$ concentration over EUS through fire-climate interactions that vary on a

445 regional scale. Moreover, the above discussed dynamical changes in future can also feedback

446 these simulated thermodynamical and precipitation changes, exaggerating the enhancement in

447 PM2.5 values over EUS in future. However, due to computational constrains, no direct

448 quantification of the magnitude of these feedback (with aerosol-radiation and aerosol-cloud

449 interactions turned off) on PM2.5 is performed and would be taken up in future studies.

450 Lastly, the reason of why the contribution of wildfire emissions to the total surface

451 PM$_{2.5}$ in EUS is so substantial in the 2050s is the drastic reduction of anthropogenic

452 contribution to the surface PM$_{2.5}$ over EUS in the future primarily due to policy-driven

453 reduction in anthropogenic emissions under the RCP4.5 scenario. Specifically, the simulated

454 ambient summer mean PM$_{2.5}$ concentration exhibits widespread declines in the future

455 (Supplementary Figure 4), with reduction in PM$_{2.5}$ concentration over eastern US in the range

456 of 4-15 $\mu g/m^3$, which is greatest within North America. Thus, large reduction in

457 anthropogenic contribution combined with increased downwind advection of Canadian

458 smoke and WUS to EUS and the associated positive feedbacks can explain the projected

459 dominance of wildfire emissions over EUS in future.
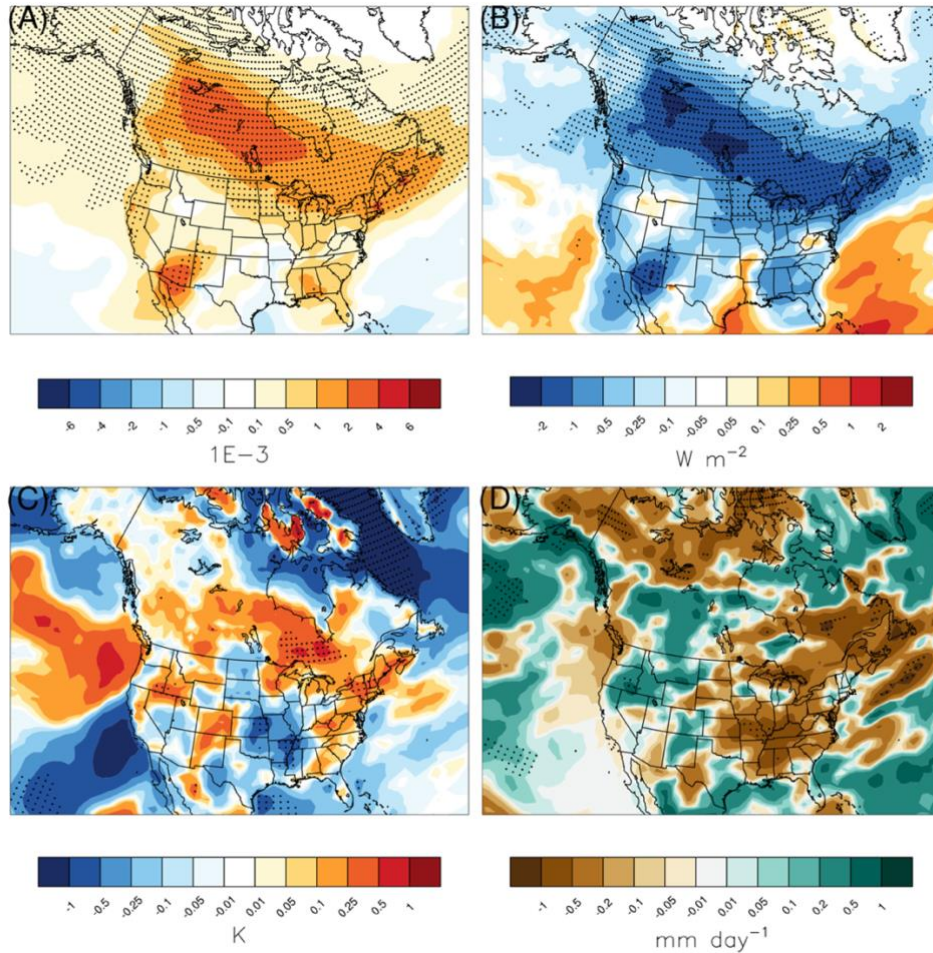
Figure 6: Spatial distribution of decadal mean summer (June through August; JJA) wildfire-induced future changes [(2050$_{ALL}$-2050$_{WEF}$) – (2000$_{ALL}$-2000$_{WEF}$)]. A) aerosol absorption optical depth at 550 nm, B) aerosol direct radiative forcing at surface, C) lower-tropospheric stability calculated as the difference between the potential temperature at 900 hPa and 1000 hPa, D) summer averaged precipitation rates, over North America. Areas marked with black dots indicate grids where changes are significant at the 95% confidence level.

3.4 Future Implications and uncertainties

However, is the simulated future enhancement in wildfire contribution over EUS

substantial enough to affect the surface PM$_{2.5}$ values over EUS in future? The World Health

Organization (WHO) air quality guidelines for annual and daily PM$_{2.5}$ concentration are 10

$\mu g\ m^{-3}$ and 25 $\mu g\ m^{-3}$, respectively. As no specific guideline for seasonal-mean PM$_{2.5}$ in the

summer is available, we use the annual guideline value as a reference to understand the

implication of wildfire emissions on ambient PM$_{2.5}$ concentration in the future. Interestingly,

475 the mean summertime PM2.5 concentration in the wildfire emission free (WEF) scenario is

476 projected to remain within $10\,\mu g\,m^{-3}$ over most of North America, except for the

477 southeastern US (~15% of the domain) (Figure 7A). However, the ALL-scenario projects an

478 increase in the exposure concentration level such that values $> 10\,\mu g/m^3$ are common in

479 Canada and EUS in the future (Figure 7B). Quantitatively, over Canada, the entire PDF of

480 PM2.5 concentration shifts towards higher values by ~5-6 $\mu g/m^3$. Specifically, the modal value

481 shifts from ~ 6 $\mu g/m^3$ in 2050WEF to 11-12 $\mu g/m^3$ in 2050ALL (Figure 7C), so PM2.5

482 concentration is projected to surpass the WHO guidelines over a large fraction of Canada in

483 the future. Similarly, the entire PDF of PM2.5 concentration shifts towards higher values by

484 ~2-3 $\mu g/m^3$ over EUS, with the mode of the PDF increasing from ~ 7-8 $\mu g/m^3$ in 2050WEF to

485 ~ 10-11 $\mu g/m^3$ in 2050ALL (Figure 7E). The modal value of summer mean PM2.5 over WUS

486 increases from ~ 6 $\mu g/m^3$ in 2050WEF to ~ 7-8 $\mu g/m^3$ in 2050ALL (Figure 7D), although a few

487 grid cells show PM2.5 values greater than 10 $\mu g/m^3$ (Figure 7B).

488   Clearly, the climate-induced enhancement in fires and its influence via the advected

489 wildfire smoke to EUS can have significant implications for air quality management in the

490 future. The PM2.5 enhancement in future over the southern states within EUS is large (Figure

491 7A-B), which is consistent with Figure 3 and 4 results. However, the future change in burnt

492 area over the same region is negligible or mostly reducing (Figure 1C-D). Thus, it can be

493 argued that the simulated enhancement is mostly related with the dynamic perturbations and

494 thermodynamical feedbacks due to wildfire emissions (Figure 6). As the rate of

495 anthropogenic emissions is also regionally highest over the Southeastern states, the impact of

496 these wildfire-induced climatic feedbacks on local air quality is distinctly seen over the EUS.

497
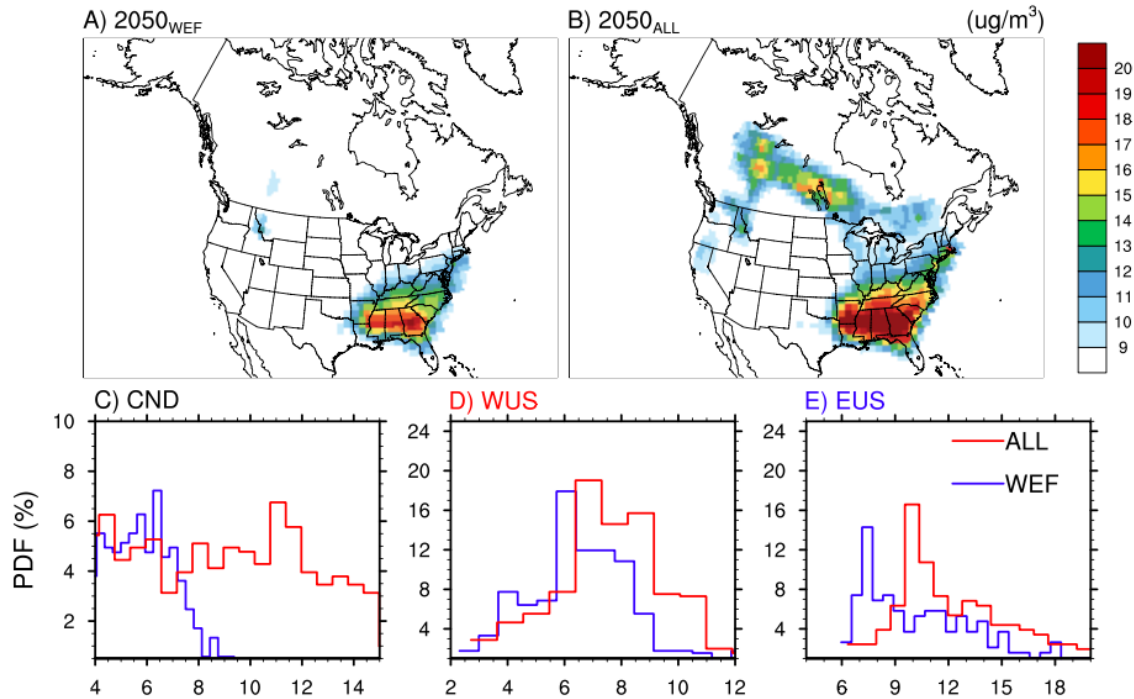
Figure 7: **Spatial distribution and probability density function of** PM2.5 **concentration in 2050s. A-B**, Spatial distribution of decadal-average summer (June through August; JJA) mean PM2.5 concentration over North America in mid-21st century from 2050WEF (wildfire emission-free) (A) and 2050ALL (wildfire emission-inclusive) (B). **C-E**, Probability density functions (PDFs) of the same within the three regions shown in Figure 2B for Canada; CND (C), western US; WUS (D), and eastern US; EUS (E), respectively, for the 2050WEF (blue) and 2050ALL (red) runs. The y-axis indicates the probability of occurrence of different PM2.5 values shown in the x-axis. Only grids over land in North America are used to generate the PDFs. Note the different ranges of values shown in the y- and x-axis in **C-E**. The colorbar and the x-axis for Panel C-E indicates PM2.5 values.

Note that our simulated present-day estimates of wildfire induced PM2.5 values as well

as the percentage contribution of wildfire emissions are within the range of reported values in

previous studies over the domain, which augment the fidelity our future projections.

Specifically, our simulated present-day estimates of wildfire induced PM2.5 values are also

within the range of reported values in previous studies over the domain. Reported values of

wildfire-induced PM2.5 over WUS during summertime vary from ~1 µg/m³ (Jaffe et al., 2008)

to ~2 µg/m³ (Park et al., 2007) and ~3 µg/m³ (Ford et al., 2018), with the highest values

documented over the Pacific Northwest and west coast regions (~1-4 µg/m³) (O'Dell et al.,

2019). The wildfire-induced PM2.5 over EUS during summertime varies from ~1 µg/m³ (Park

517   et al., 2007) to ~2.5 µg/m^3 (~ 3 µg/m^3 in the southeastern US) (Ford et al., 2018).

518   Consistently, our simulated present-day estimates of wildfire contribution values are also

519   within the range of reported values in previous studies. For example, Meng et al. (2019)

520   found that wildfires can be the largest sectoral contributor (~18-59%) to the population-

521   weighted PM$_{2.5}$ in various subregions of Canada. Over WUS, the present-day percentage

522   contribution of wildfire induced PM$_{2.5}$ to the total PM$_{2.5}$ is reported to be ~ 12% (Liu et al.,

523   2017), ~ 15% (Park et al., 2007) and ~30% (Ford et al., 2018), with higher values of ~40% in

524   the Pacific Northwest (O'Dell et al., 2019). Over EUS our simulated values are also within

525   the range of previously reported values of ~ 5% (Park et al., 2007) and ~15-18% (Ford et al.,

526   2018). However, our two-way coupled simulations illustrate that future enhancement in the

527   wildfire associated PM$_{2.5}$ over the EUS could be greater compared to the western US, which

528   is not emphasized explicitly in any of the previous studies (although Ford et al., 2018

529   illustrated increase in PM2.5 over mid and central US from Canadian fires). These could be

530   since inclusion of the wildfire-induced climatic feedbacks in our simulation is an

531   unprecedented exercise. Please also note that our study is focused on JJA period and the

532   wildfires in western US mainly occurs during August-September months, so the results

533   should be compared consciously.

534   Nonetheless, inherent limitations in our simulations may introduce uncertainties in the

535   projected future changes. For example, our reported changes in PM$_{2.5}$ concentrations based on

536   relatively coarse resolution simulations and decadal averages likely represent a low-end

537   estimate compared to changes at regional and daily/weekly scales. Moreover, our

538   experiments do not consider the direct human influences such as population change and

539   socioeconomic development on wildfires, which may aggravate the increase in PM$_{2.5}$

540   concentrations over the densely populated EUS in the future. Common sources of uncertainty

541   in modeling burnt area and fire emission and fire aerosol and smoke are also present in our

542   model. Fire smoke, in particular, is extremely hard to measure and evaluate. Lastly, inherent

543   uncertainties in the physics parameterizations used in the model, sensitivity of climate to

544   GHGs emissions, and the RCP scenarios should also be noted. Thus, ensemble modeling

545   considering different emissions scenarios, population and future time periods, and the use of

546   a finer spatial resolution may provide a more robust and better quantification of the wildfire-

547   induced impact on policy regulated improvements in $PM_{2.5}$ over EUS.

548   **4. Conclusion**

549   In summary, online coupled fire-climate-ecosystem simulations project a nearly

550   twofold increase in wildfire-induced summer-mean surface $PM_{2.5}$ concentration by the mid-

551   21st century over the entire North America. In a wildfire-emission free future, a large portion

552   of North America will have $PM_{2.5}$ values below the WHO guidelines. But in a future with

553   wildfire emissions, the improvements from policy-driven reductions in anthropogenic $PM_{2.5}$

554   will be compromised by the projected doubling of $PM_{2.5}$ from wildfires. More strikingly,

555   wildfire-induced enhancement in surface $PM_{2.5}$ values and percentage contribution of the

556   wildfire emissions over EUS could be substantial by mid-century. This is mainly because of

557   the large enhancement in fires over Northern America by 2050s and associated increase in

558   amount of downwind transport of smoke to EUS. In addition, enhancement of smoke

559   transport induces a positive climate feedback to $PM_{2.5}$ concentrations over EUS by increasing

560   the lower-tropospheric stability and reducing wet scavenging rates. Despite the inherent

561   limitations, this study highlights the natural versus anthropogenic contributions and the non-

562   local nature of air pollution that can complicate regulatory strategies aimed at improving air

563   quality over the eastern US in a warmer future.

564

565

Data availability statements

The HMS data used in this paper are available free through the link
https://www.ospo.noaa.gov/Products/land/hms.html. The model simulations data are
available at https://portal.nersc.gov/project/m1660/yang560/wildfire

Code availability statements

The model code and scripts are available at
https://portal.nersc.gov/project/m1660/yang560/wildfire

Acknowledgements:

This research was performed at PNNL and funded under Assistance Agreement No.
RD835871 by the U.S. Environmental Protection Agency to Yale University through the
SEARCH (Solutions for Energy, AiR, Climate, and Health) Center. It has not been formally
reviewed by EPA. The views expressed in this document are solely those of the SEARCH
Center and do not necessarily reflect those of the Agency. EPA does not endorse any
products or commercial services mentioned in this publication. CS is supported by the New
Faculty Initiation Grant project number CE/20-21/065/NFIG/008961 from IIT Madras.
PNNL is operated by Battelle Memorial Institute for the U.S. Department of Energy under
contract DE-AC06-76RLO-1830.

Authors Contribution

YQ, CS and RL designed this study. CS did the model and satellite analysis and wrote the
first draft of the manuscript. YZou performed the simulations. All authors provided inputs
throughout the study and helped in the drafting and submission process.

References

Abatzoglou, J. T. and Williams, A. P.: Impact of anthropogenic climate change on wildfire
across western US forests, Proc. Natl. Acad. Sci., 113(42), 11770 LP – 11775,
doi:10.1073/pnas.1607171113, 2016.

Andela, N., Morton, D. C., Giglio, L., Chen, Y., van der Werf, G. R., Kasibhatla, P. S.,
DeFries, R. S., Collatz, G. J., Hantson, S., Kloster, S., Bachelet, D., Forrest, M., Lasslop, G.,
Li, F., Mangeon, S., Melton, J. R., Yue, C. and Randerson, J. T.: A human-driven decline in
global burned area, Science (80-.)., 356(6345), 1356 LP – 1362,
doi:10.1126/science.aal4108, 2017.

Anjali, H., Muhammad, A., Anthony, D. M., Karen, S., R., S. M., Mick, M., M., T. A., J., A.
M. and Martine, D.: Impact of Fine Particulate Matter (PM$_{2.5}$) Exposure During Wildfires on
Cardiovascular Health Outcomes, J. Am. Heart Assoc., 4(7), e001653,
doi:10.1161/JAHA.114.001653, 2019.

Black, C., Tesfaigzi, Y., Bassein, J. A. and Miller, L. A.: Wildfire smoke exposure and
human health: Significant gaps in research for a growing public health issue, Environ.

Toxicol. Pharmacol., 55, 186–195, doi:https://doi.org/10.1016/j.etap.2017.08.022, 2017.

Brey, S. J., Ruminski, M., Atwood, S. A. and Fischer, E. V: Connecting smoke plumes to sources using Hazard Mapping System (HMS) smoke and fire location data over North America, Atmos. Chem. Phys., 18(3), 1745–1761, doi:10.5194/acp-18-1745-2018, 2018.

Dempsey, F.: Forest Fire Effects on Air Quality in Ontario: Evaluation of Several Recent Examples, Bull. Am. Meteorol. Soc., 94(7), 1059–1064, doi:10.1175/BAMS-D-11-00202.1, 2013.

Dominici, F., Peng, R. D., Bell, M. L., Pham, L., McDermott, A., Zeger, S. L. and Samet, J. M.: Fine Particulate Air Pollution and Hospital Admission for Cardiovascular and Respiratory Diseases, JAMA, 295(10), 1127–1134, doi:10.1001/jama.295.10.1127, 2006.

Diao, M., Holloway, T., Choi, S., O'Neill, S.M., Al-Hamdan, M.Z., Van Donkelaar, A., Martin, R.V., Jin, X., Fiore, A.M., Henze, D.K. and Lacey, F., 2019. Methods, availability, and applications of PM2. 5 exposure estimates derived from ground measurements, satellite, and atmospheric models. *Journal of the Air & Waste Management Association*, *69*(12), pp.1391-1414.

Ford, B., Val Martin, M., Zelasky, S. E., Fischer, E. V, Anenberg, S. C., Heald, C. L. and Pierce, J. R.: Future Fire Impacts on Smoke Concentrations, Visibility, and Health in the Contiguous United States, GeoHealth, 2(8), 229–247, doi:10.1029/2018GH000144, 2018.

Gillett, N. P., Weaver, A. J., Zwiers, F. W. and Flannigan, M. D.: Detecting the effect of climate change on Canadian forest fires, Geophys. Res. Lett., 31(18), doi:10.1029/2004GL020876, 2004.

Gunsch, M. J., May, N. W., Wen, M., Bottenus, C. L. H., Gardner, D. J., VanReken, T. M., Bertman, S. B., Hopke, P. K., Ault, A. P. and Pratt, K. A.: Ubiquitous influence of wildfire emissions and secondary organic aerosol on summertime atmospheric aerosol in the forested Great Lakes region, Atmos. Chem. Phys., 18(5), 3701–3715, doi:10.5194/acp-18-3701-2018, 2018.

Guan S, Wong DC, Gao Y, Zhang T, Pouliot G. Impact of wildfire on particulate matter in the southeastern United States in November 2016. Sci Total Environ. 2020;724:138354. doi:10.1016/j.scitotenv.2020.138354.

Johnston F. H., Henderson. S. B., Yang, C., T., R. J., Miriam, M., S., D. R., Patrick, K., M.J.S., B. D. and Michael, B.: Estimated Global Mortality Attributable to Smoke from Landscape Fires, Environ. Health Perspect., 120(5), 695–701, doi:10.1289/ehp.1104422, 2012.

Harris, R. M. B., Remenyi, T. A., Williamson, G. J., Bindoff, N. L., and Bowman, D. M. J. S.: Climate-vegetation fire interactions and feedbacks: trivial detail or major barrier to projecting the future of the Earth system?, Wires Clim. Change, 7, 910-931, 10.1002/wcc.428, 2016.

Hantson, S., Arneth, A., Harrison, S. P., Kelley, D. I., Prentice, I. C., Rabin, S. S., et al. (2016). The status and challenge of global fire modelling. Biogeosciences, 13, 3359–3375. https://doi.org/10.5194/bg-13-3359-2016

Hu, X., Yu, C., Tian, D., Ruminski, M., Robertson, K., Waller, L. A. and Liu, Y.: Comparison of the Hazard Mapping System (HMS) fire product to ground-based fire records

647   in Georgia, USA, J. Geophys. Res. Atmos., 121(6), 2901–2910, doi:10.1002/2015JD024448,
648   2016.

649   HURTT, G. C., FROLKING, S., FEARON, M. G., MOORE, B., SHEVLIAKOVA, E.,
650   MALYSHEV, S., PACALA, S. W. and HOUGHTON, R. A.: The underpinnings of land-use
651   history: three centuries of global gridded land-use transitions, wood-harvest activity, and
652   resulting secondary lands, Glob. Chang. Biol., 12(7), 1208–1229, doi:10.1111/j.1365-
653   2486.2006.01150.x, 2006.

654   Jaffe, D., Hafner, W., Chand, D., Westerling, A. and Spracklen, D.: Interannual Variations in
655    $PM_{2.5}$ due to Wildfires in the Western United States, Environ. Sci. Technol., 42(8), 2812–
656   2818, doi:10.1021/es702755v, 2008.

657   Jolly, W. M., Cochrane, M. A., Freeborn, P. H., Holden, Z. A., Brown, T. J., Williamson, G.
658   J. and Bowman, D. M. J. S.: Climate-induced variations in global wildfire danger from 1979
659   to 2013, Nat. Commun., 6, 7537 [online] Available from:
660   https://doi.org/10.1038/ncomms8537, 2015.

661   Kaulfus, A. S., Nair, U., Jaffe, D., Christopher, S. A. and Goodrick, S.: Biomass Burning
662   Smoke Climatology of the United States: Implications for Particulate Matter Air Quality,
663   Environ. Sci. Technol., 51(20), 11731–11741, doi:10.1021/acs.est.7b03292, 2017.

664   Kirchmeier-Young, M. C., Zwiers, F. W., Gillett, N. P. and Cannon, A. J.: Attributing
665   extreme fire risk in Western Canada to human emissions, Clim. Change, 144(2), 365–379,
666   doi:10.1007/s10584-017-2030-0, 2017.

667   Kitzberger, T., Falk, D. A., Westerling, A. L. and Swetnam, T. W.: Direct and indirect
668   climate controls predict heterogeneous early-mid 21st century wildfire burned area across
669   western and North America, PLoS One, 12(12), e0188486 [online] Available from:
670   https://doi.org/10.1371/journal.pone.0188486, 2017.

671   Knorr, W., Dentener, F., Lamarque, J.-F., Jiang, L. and Arneth, A.: Wildfire air pollution
672   hazard during the 21st century, Atmos. Chem. Phys., 17(14), 9223–9236, doi:10.5194/acp-
673   17-9223-2017, 2017.

674   Koplitz, S.N., Nolte, C.G., Pouliot, G.A., Vukovich, J.M. and Beidler, J., 2018. Influence of
675   uncertainties in burned area estimates on modeled wildland fire PM2. 5 and ozone pollution
676   in the contiguous US. *Atmospheric environment*, *191*, pp.328-339.

677   Lamarque, J. F., Bond, T. C., Eyring, V., Granier, C., Heil, A., Klimont, Z., Lee, D., Liousse,
678   C., Mieville, A., Owen, 628 B., Schultz, M. G., Shindell, D., Smith, S. J., Stehfest, E., Van
679   Aardenne, J., Cooper, O. R., Kainuma, M., 629 Mahowald, N., McConnell, J. R., Naik, V.,
680   Riahi, K., and van Vuuren, D. P.: Historical (1850-2000) gridded anthropogenic and biomass
681   burning emissions of reactive gases and aerosols: methodology and application, 631 Atmos.
682   Chem. Phys., 10, 7017-7039, 10.5194/acp-10-7017-2010, 2010.

683   Leibensperger, E. M., Mickley, L. J., Jacob, D. J., Chen, W.-T., Seinfeld, J. H., Nenes, A.,
684   Adams, P. J., Streets, D. G., Kumar, N. and Rind, D.: Climatic effects of 1950–2050
685   changes in US anthropogenic aerosols – Part 2: Climate response, Atmos. Chem.
686   Phys., 12(7), 3349–3362, doi:10.5194/acp-12-3349-2012, 2012.

687   Li, F., Zeng, X. D., & Levis, S. (2012). A process-based fire parameterization of intermediate
688   complexity in a dynamic global vegetation model. Biogeosciences, 9(7), 2761–2780.
689   https://doi.org/10.5194/bg-9-2761-2012

Liu, J. C., Mickley, L. J., Sulprizio, M. P., Dominici, F., Yue, X., Ebisu, K., Anderson, G. B., Khan, R. F. A., Bravo, M. A. and Bell, M. L.: Particulate Air Pollution from Wildfires in the Western US under Climate Change, Clim. Change, 138(3), 655–666, doi:10.1007/s10584-016-1762-6, 2016.

Liu, Y., Goodrick, S. and Heilman, W.: Wildland fire emissions, carbon, and climate: Wildfire–climate interactions, For. Ecol. Manage., 317, 80–96, doi:https://doi.org/10.1016/j.foreco.2013.02.020, 2014.

Liu, X., Easter, R. C., Ghan, S. J., Zaveri, R., Rasch, P., Shi, X., Lamarque, J. F., Gettelman, A., Morrison, H., Vitt, F., Conley, A., Park, S., Neale, R., Hannay, C., Ekman, A. M. L., Hess, P., Mahowald, N., Collins, W., Iacono, M. J., Bretherton, C. S., Flanner, M. G., and Mitchell, D.: Toward a minimal representation of aerosols in climate models: description and evaluation in the Community Atmosphere Model CAM5, Geosci. Model Dev., 5, 709- 652 739, 10.5194/gmd-5-709-2012, 2012.

Meng, J., Martin, R.V., Li, C., van Donkelaar, A., Tzompa-Sosa, Z.A., Yue, X., Xu, J.W., Weagle, C.L. and Burnett, R.T., 2019. Source Contributions to Ambient Fine Particulate Matter for Canada. *Environmental science & technology*, *53*(17), pp.10269-10278.

McClure, C. D. and Jaffe, D. A.: US particulate matter air quality improves except in wildfire-prone areas, Proc. Natl. Acad. Sci., 115(31), 7901 LP – 7906, doi:10.1073/pnas.1804353115, 2018.

Neale, R. B., Chen, C. C., Gettelman, A., Lauritzen, P. H., Park, S., Williamson, D. L., Conley, A. J., Garcia, R., Kinnison, D., Lamarque, J. F., Marsh, D., Mills, M., Smith, A. K., Tilmes, S., Vitt, F., Morrison, H., Cameron671 Smith, P., Collins, W. D., Iacono, M. J., Easter, R. C., Ghan, S. J., Liu, X. H., Rasch, P. J., and Taylor, M. A.: Description of the NCAR Community Atmosphere Model (CAM 5.0), NCAR 289, 2013

Nolte, C. G., Spero, T. L., Bowden, J. H., Mallard, M. S. and Dolwick, P. D.: The potential effects of climate change on air quality across the conterminous US at 2030 under three Representative Concentration Pathways, Atmos. Chem. Phys., 18(20), 15471–15489, doi:10.5194/acp-18-15471-2018, 2018.

Katelyn O'Dell, Bonne Ford, Emily V. Fischer, and Jeffrey R. Pierce Environmental Science & Technology 2019 53 (4), 1797-1804, DOI: 10.1021/acs.est.8b05430.

Partain, J. L., Alden, S., Strader, H., Bhatt, U. S., Bieniek, P. A., Brettschneider, B. R., Walsh, J. E., Lader, R. T., Olsson, P. Q., Rupp, T. S., Thoman, R. L., York, A. D. and Ziel, R. H.: An Assessment of the Role of Anthropogenic Climate Change in the Alaska Fire Season of 2015, Bull. Am. Meteorol. Soc., 97(12), S14–S18, doi:10.1175/BAMS-D-16-0149.1, 2016.

Park, S., Bretherton, C. S., and Rasch, P. J.: Integrating Cloud Processes in the Community Atmosphere Model, Version 5, J. Climate, 27, 6821-6856, 10.1175/Jcli-D-14-00087.1, 2014.

Park, R.J., Jacob, D.J. and Logan, J.A., 2007. Fire and biofuel contributions to annual mean aerosol mass concentrations in the United States. *Atmospheric Environment*, *41*(35), pp.7389-7400.

Pierce, J. R., Val Martin, M., & Heald, C. L. (2017). Estimating the Effects of Changing Climate on Fires and Consequences for U.S. Air Quality, Using a Set of Global and Regional Climate Models (final report no. JFSP-13-1-01-4). Retrieved from

734   https://www.firescience.gov/projects/ 13-1-01-4/project/13-1-01-4_final_report.pdf

735   Pouliot G, Pace TG, Roy B, Pierce T, Mobley D. Development of a biomass burning
736   emissions inventory by combining satellite and ground-based information. J Appl Remote
737   Sens. 2008;2:021501. doi: 10.1117/1.2939551.

738   Randerson, J. T., Chen, Y., van der Werf, G. R., Rogers, B. M., & Morton, D. C. (2012).
739   Global burned area and biomass burning emissions from small fires. Journal of Geophysical
740   Research, 117, G04012. https://doi.org/10.1029/2012JG002128

741   Rolph, G. D., Draxler, R. R., Stein, A. F., Taylor, A., Ruminski, M. G., Kondragunta, S.,
742   Zeng, J., Huang, H.-C., Manikin, G., McQueen, J. T. and Davidson, P. M.: Description and
743   Verification of the NOAA Smoke Forecasting System: The 2007 Fire Season, Weather
744   Forecast., 24(2), 361–378, doi:10.1175/2008WAF2222165.1, 2009.

745   Spracklen, D. V., Mickley, L. J., Logan, J. A., Hudman, R. C., Yevich, R., Flannigan, M. D.,
746   & Westerling, A. L. (2009). Impacts of climate change from 2000 to 2050 on wildfire activity
747   and carbonaceous aerosol concentrations in the western United States. Journal of Geophysical
748   Research, 114, D20301. https://doi.org/10.1029/2008JD010966

749   Sun, Y., Gu, L. H., and Dickinson, R. E.: A numerical issue in calculating the coupled carbon
750   and water fluxes in a climate model, J. Geophys. Res.-Atmos., 117,
751   D2210310.1029/2012jd018059, 2012

752   Sofiev, M., Ermakova, T., and Vankevich, R.: Evaluation of the smoke-injection height from
753   wild-land fires using remote-sensing data, Atmos. Chem. Phys., 12, 1995-2006, 10.5194/acp-
754   12-1995-2012, 2012

755   Shi, H., Jiang, Z., Zhao, B., Li, Z., Chen, Y., Gu, Y., Jiang, J. H., Lee, M., Liou, K.-N., Neu,
756   J. L., Payne, V. H., Su, H., Wang, Y., Witek, M. and Worden, J.: Modeling Study of the Air
757   Quality Impact of Record-Breaking Southern California Wildfires in December 2017, J.
758   Geophys. Res. Atmos., 0(0), doi:10.1029/2019JD030472, 2019.

759   U.S. EPA (U.S. Environmental Protection Agency). 2009. Integrated Science Assessment
760   (ISA) For Particulate Matter (Final Report). EPA/600/R-08/139F.Washington, DC:U.S. EPA.

761   U.S. EPA. 2018. Our Nation's Air. https://gispub.epa.gov/air/trendsreport/2018/

762   Val Martin, M., Heald, C. L., Lamarque, J.-F., Tilmes, S., Emmons, L. K. and Schichtel, B.
763   A.: How emissions, climate, and land use change will impact mid-century air quality over the
764   United States: a focus on effects at national parks, Atmos. Chem. Phys., 15(5), 2805–2823,
765   doi:10.5194/acp-15-2805-2015, 2015.

766   Van der Werf, G. R., Randerson, J. T., Giglio, L., Collatz, G. J., Kasibhatla, P. S., and
767   Arellano, A. F.: Interannual variability in global biomass burning emissions from 1997 to
768   2004, Atmos. Chem. Phys., 6, 3423-3441, DOI 737 10.5194/acp-6-3423-2006, 2006

769   Van Der Werf, G. R., Randerson, J. T., Giglio, L., Collatz, G. J., Mu, M., Kasibhatla, P. S.,
770   Morton, D. C., Defries, R. S., Jin, Y. and Van Leeuwen, T. T.: Global fire emissions and the
771   contribution of deforestation, savanna, forest, agricultural, and peat fires (1997-2009), Atmos.
772   Chem. Phys., 10(23), 11707–11735, doi:10.5194/acp-10-11707-2010, 2010.

773   Van Donkelaar, A., R. V. Martin, M. Brauer, N. C. Hsu, R. A. Kahn, R. C. Levy, A.
774   Lyapustin, A. M. Sayer, and D. M. Winker. 2018. Global Annual $PM_{2.5}$ Grids from MODIS,
775   MISR and SeaWiFS Aerosol Optical Depth (AOD) with GWR, 1998-2016. Palisades NY:

776 NASA Socioeconomic Data and Applications Center (SEDAC).
777 https://doi.org/10.7927/H4ZK5DQS. Accessed 16 November 2019.

778 Ward, D. S., Kloster, S., Mahowald, N. M., Rogers, B. M., Randerson, J. T. and Hess, P. G.:
779 The changing radiative forcing of fires: global model estimates for past, present and future,
780 Atmos. Chem. Phys., 12(22), 10857–10886, doi:10.5194/acp-12-10857-2012, 2012.

781 Wotton, B. M., Flannigan, M. D., and Marshall, G. A.: Potential climate change impacts on
782 fire intensity and key wildfire suppression thresholds in Canada, Environ. Res. Lett., 12,
783 095003, https://doi.org/10.1088/1748-9326/aa7e6e, 2017.

784 Westerling, A. L., Hidalgo, H. G., Cayan, D. R. and Swetnam, T. W.: Warming and Earlier
785 Spring Increase Western U.S. Forest Wildfire Activity, Science (80-.)., 313(5789), 940 LP –
786 943, doi:10.1126/science.1128834, 2006.

787 Wotawa, G. and Trainer, M.: The Influence of Canadian Forest Fires on Pollutant
788 Concentrations in the United States, Science (80-.)., 288(5464), 324 LP – 328,
789 doi:10.1126/science.288.5464.324, 2000.

790 Wu, Y., Arapi, A., Huang, J., Gross, B. and Moshary, F.: Intra-continental wildfire smoke
791 transport and impact on local air quality observed by ground-based and satellite remote
792 sensing in New York City, Atmos. Environ., 187, 266–281,
793 doi:https://doi.org/10.1016/j.atmosenv.2018.06.006, 2018.

794 Xue, Z., Gupta, P., and Christopher, S.: Satellite-based estimation of the impacts of
795 summertime wildfires on PM2.5concentration in the United States, Atmos. Chem. Phys., 21,
796 11243–11256, https://doi.org/10.5194/acp-21-11243-2021, 2021.

797 Yang, P.-L., Y. Zhang, K. Wang, P. Doraiswamy, and S.-H. Cho, 2019, Health Impacts and
798 Cost-Benefit Analyses of Surface O_3 and $PM_{2.5}$ over the U.S. under Future Climate and
799 Emission Scenarios, *Environmental Research*, 178, November 2019, 108687,
800 https://doi.org/10.1016/j.envres.2019.108687.

801 Yue, X., Mickley, L. J., Logan, J. A. and Kaplan, J. O.: Ensemble projections of wildfire
802 activity and carbonaceous aerosol concentrations over the western United States in the mid-
803 21st century, Atmos. Environ., 77, 767–780,
804 doi:https://doi.org/10.1016/j.atmosenv.2013.06.003, 2013.

805 Zou, Y., Wang, Y., Ke, Z., Tian, H., Yang, J. and Liu, Y.: Development of a REgion-Specific
806 Ecosystem Feedback Fire (RESFire) Model in the Community Earth System Model, J. Adv.
807 Model. Earth Syst., 11(2), 417–445, doi:10.1029/2018MS001368, 2019.

808 Zou, Y., Wang, Y., Qian, Y., Tian, H., Yang, J. and Alvarado, E.: Using CESM-RESFire to
809 understand climate–fire–ecosystem interactions and the implications for decadal climate
810 variability, Atmos. Chem. Phys., 20, 995–1020, https://doi.org/10.5194/acp-20-995-2020,
811 2020.

812 Zhang, Y., P.-L. Yang, Y. Gao, R. L. Leung, and M. Bell, 2020, Health and Economic
813 Impacts of Air Pollution Induced by Climate Extremes over the Continental U.S.,
814 *Environmental International*, 143, 105921, https://doi.org/10.1016/j.envint.2020.105921.

815

816